A new mechanistic model for an O 2-protected electron-bifurcating hydrogenase, Hnd from Desulfovibrio fructosovorans

Arlette Kpebe, Martino Benvenuti, Chloé Guendon, Amani Rebai, Victoria Fernandez, Sébastien Le Laz, Emilien Etienne, Bruno Guigliarelli, Gabriel García-Molina, Antonio L de Lacey, et al.

A new mechanistic model for an O_2-protected electron-bifurcating hydrogenase, Hnd from *Desulfovibrio fructosovorans*

Arlette Kpebe[a], Martino Benvenuti[a], Chloé Guendon[a], Amani Rebai[a], Victoria Fernandez[a], Sébastien Le Laz[a], Emilien Etienne[a], Bruno Guigliarelli[a], Gabriel García-Molina[b], Antonio L. de Lacey[b], Carole Baffert[a]* and Myriam Brugna[a]*

[a]Aix Marseille Univ, CNRS, BIP, 31 Chemin Joseph Aiguier, 13402, Marseille cedex 09, France
[b]Instituto de Catálisis y Petroleoquímica, CSIC, c/ Marie Curie 2, Madrid, Spain

* Correspondence to: Myriam Brugna, E-mail: mbrugna@imm.cnrs.fr; phone: +33491164568
Carole Baffert, E-mail: cbaffert@imm.cnrs.fr; phone : +33491164541
Laboratoire de Bioénergétique et Ingénierie des Protéines, Aix Marseille Univ, CNRS, 31 Chemin Joseph Aiguier, CS 70071, 13402 Marseille cedex 09, France

Email :
akpebe@imm.cnrs.fr
mbenvenuti@imm.cnrs.fr
cguendon@imm.cnrs.fr
amani.rebai93@gmail.com
victoriafernandez@hotmail.fr
sebastien.le-laz@laposte.net
eetienne@imm.cnrs.fr
guigliar@imm.cnrs.fr
gabriel.garcia.m@csic.es
alopez@icp.csic.es
cbaffert@imm.cnrs.fr
mbrugna@imm.cnrs.fr

Keywords: Hydrogenase, electron bifurcation, ferredoxin, flavin, *Desulfovibrio*

Abstract

The genome of the sulfate-reducing and anaerobic bacterium *Desulfovibrio fructosovorans* encodes different hydrogenases. Among them is Hnd, a tetrameric cytoplasmic [FeFe] hydrogenase that has previously been described as an NADP-specific enzyme (Malki et al., 1995). In this study, we purified and characterized a recombinant Strep-tagged form of Hnd and demonstrated that it is an electron-bifurcating enzyme. Flavin-based electron-bifurcation is a mechanism that couples an exergonic redox reaction to an endergonic one allowing energy conservation in anaerobic microorganisms. One of the three ferredoxins of the bacterium, that was named FdxB, was also purified and characterized. It contains a low-potential (E_m = -450 mV) [4Fe4S] cluster. We found that Hnd was not able to reduce $NADP^+$, and that it catalyzes the simultaneous reduction of FdxB and NAD^+. Moreover, Hnd is the first electron-bifurcating hydrogenase that retains activity when purified aerobically due to formation of an inactive state of its catalytic site protecting against O_2 damage (H_{inact}). Hnd is highly active with the artificial redox partner (methyl viologen) and can perform the electron-bifurcation reaction to oxidize H_2 with a specific activity of 10 µmol of NADH/min/mg of enzyme. Surprisingly, the ratio between NADH and reduced FdxB varies over the reaction

with a decreasing amount of FdxB reduced per NADH produced, indicating a more complex mechanism than previously described. We proposed a new mechanistic model in which the ferredoxin is recycled at the hydrogenase catalytic subunit.

1. Introduction

Hydrogenases are enzymes able to catalyze in a reversible way both the oxidation of molecular hydrogen and the reduction of protons. They have been divided into two main classes, depending on the metal content in the active site, [FeFe] and [NiFe] hydrogenases [1, 2]. The [FeFe] and [NiFe] active sites have in common the presence of carbon monoxide (CO) and cyanide groups (CN^-) bound to the iron ions [3]. In addition, these enzymes contain FeS clusters providing an electron transfer chain between the catalytic site and electron donors or acceptors [4]. These enzymes are very diverse and widespread in Bacteria and Archaea but only few representatives are characterized in depth [5].
Recently, a novel group of hydrogenases capable of electron bifurcation was described [6-10]. Flavin-based electron bifurcation is a newly discovered mechanism of biological energy conservation that simultaneously couples an endergonic redox reaction to an exergonic redox reaction [11]. The electron-bifurcating enzymes that have been characterized so far contain at least one flavin-containing subunit and iron-sulfur clusters, excepted the bifurcating butyryl-CoA dehydrogenase (Bcd)-electron transferring flavoprotein (Etf) system that does not contain iron-sulfur cluster [12]. They catalyze a ferredoxin (Fd) or a flavodoxin-dependent reaction and can be divided into four families that have evolved independently, among them a family of enzymes containing a NuoF homolog (NADH-binding subunit of NADH:quinone oxidoreductase from *Escherichia coli*) which includes hydrogenases [11, 13, 14]. Flavin-based electron bifurcating hydrogenases are trimeric or tetrameric, soluble, of [FeFe]-type and contain, in addition to the hydrogenase subunit harboring the catalytic H-cluster, a [2Fe2S] containing subunit and the NuoF homolog which is the FMN- and FeS-containing NADH binding subunit [13-15]. Representatives were isolated from the anaerobic bacteria *Thermotoga maritima* [6], *Acetobacterium woodii* [7], *Moorella thermoacetica* [9], and *Ruminococcus albus* [10]. They catalyze the simultaneous exergonic oxidation of the Fd and the endergonic oxidation of NADH to produce H_2 (electron confurcation) [6], the reverse reaction in which the exergonic reduction of NAD^+ is coupled to the endergonic reduction of the Fd in the presence of dihydrogen (electron bifurcation) [7] (eq 1) or the reaction in both directions [8-10].

$$Fd_{ox} + NAD^+ + 2H_2 = Fd_{red}^{2-} + NADH + 3H^+ \qquad \text{eq 1}$$

In *Clostridium autoethanogenum*, an NADP-specific electron-bifurcating [FeFe] hydrogenase is present and forms a complex with a formate dehydrogenase [8].

Genes encoding hydrogenases highly similar to electron-bifurcating hydrogenases are present in *Desulfovibrio* species. *Desulfovibrio* are sulfate-reducing bacteria that can alternatively use molecular hydrogen as the sole source of electron and energy for their growth or produce H_2 when growing fermentatively [16, 17]. *Desulfovibrio fructosovorans*, our model organism, is able to degrade fructose [18] and possesses a complex hydrogenase system composed of several enzymes with different subunit composition and cellular localization, among them the periplasmic dimeric [NiFe] hydrogenase Hyn [19, 20] which has been extensively studied at the molecular level [21, 22], the periplasmic dimeric [FeFe] hydrogenase Hyd [23], and the cytoplasmic [FeFe] hydrogenase Hnd [24].
The four proteins encoded by the *hnd* operon [25] were demonstrated, using antisera, to form a heterotetrameric complex [26] (see Figure 1 for a schematic representation of the tetrameric

complex). HndA contains a [2Fe2S] cluster ligated by four cysteine residues (Figure S1) that was characterized by EPR spectroscopy and can transfer electrons to the FeS cluster located in the HndD N-terminal domain [27, 28]. The structure of its C-terminal domain was determined by NMR [29]: it consists of a thioredoxin-like domain where the [2Fe2S] cluster is surface exposed and contains the interaction site with the N-terminal domain of HndD. HndB's function is unknown but it was proposed to bind an unusual [2Fe2S] cluster coordinated by three cysteine and one serine residues [28] (Figure S2). Based on its sequence, HndC was predicted to harbour binding sites for a flavin (FMN) and for NAD(P) and to coordinate three [4Fe4S] clusters [25] (Figure S3). A second flavin site was proposed by Buckel and Thauer [13, 14] although it cannot be deduced from sequence subunits. HndD, the hydrogenase catalytic subunit, presents 40% sequence identity with CpI, the well-characterized monomeric [FeFe] hydrogenase from *Clostridium pasteurianum* [25, 30]. It harbors the cysteine residues to accommodate the H-cluster, the active site, one [2Fe2S] cluster and two conventional [4Fe4S] clusters as well as a non-conventional [4Fe4S] cluster that might be ligated by three cysteine and one histidine residues as in CpI from *C. pasteurianum* [31] (Figure S4).

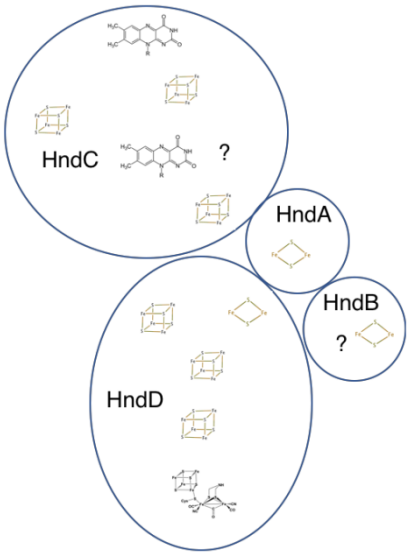

Figure 1: Schematic representation of the heterotetrameric complex of Hnd composed of HndA, HndB, HndC and HndD subunits. The cofactors are predicted from amino acid sequence analysis [25]. The presence of a [2Fe2S] cluster in HndB is uncertain because the cluster binding motif is not conserved [28]. The proposed Y-shaped arrangement of cofactors in HndD is based on the analogy with clostridial hydrogenases [31, 32]. The cofactors arrangement in HndA, B and C and the subunits arrangement are speculative except the one of HndA which has been shown to interact with HndD [28].

Hnd hydrogenase was described as an $NADP^+$-reducing hydrogenase [25, 26]. Indeed, in cell extracts, a H_2 dependent $NADP^+$-reducing activity was observed which was completely abolished in *hndC* or *hndD* deletion mutant strains whereas no H_2-induced NAD^+ reduction was observed in the WT strain. The purification of the native Hnd enzyme was not possible because of its low representativity in cells [26].

Here we describe the cloning, production and purification of a recombinant form of the tetrameric Hnd hydrogenase of *D. fructosovorans* and report its properties. We demonstrate that this enzyme is part of the electron-bifurcating hydrogenase class. Surprisingly, Hnd is a NAD^+-dependent enzyme and not a $NADP^+$-dependent enzyme as previously described [25, 27]. Our results show that Hnd is the first electron-bifurcating hydrogenase that retains activity when aerobically purified. It reduces simultaneously NAD^+ and a low-potential [4Fe4S] cluster containing Fd, in a bifurcating reaction but is also able to

reduce NAD^+ in the absence of Fd with a lower specific activity. Moreover, during electron-bifurcating reaction, Hnd produces less reduced Fd than NADH, indicating a more complex mechanism than previously described.

2. Materials and methods

2.1. Bacterial strains and plasmids

All strains and plasmids used in the present study are listed in Table 1. *Escherichia coli* DH5α and JM109 were used as hosts for recombinant plasmid construction. All primers used in this study are listed in Table 2.

Table 1: Strains and plasmids used in the present study.

Bacterial strain or plasmid	**Relevant characteristic**	**Reference or source**
Bacterial strains		
E.coli ΔiscR	MG1655 Δ*iscR::kan*	This work
E.coli JM109	F´ traD36 proA+B+ lacIq Δ(lacZ)M15/ Δ(lac-proAB) glnV44 e14- gyrA96 recA1 relA1 endA1 thi hsdR17	NEB
E.coli DH5α	F– Φ80*lac*ZΔM15 Δ(*lac*ZYA-*arg*F)U169 *rec*A1 *end*A1 *hsd*R17 (rK–, mK+) *pho*A *sup*E44 *thi*-1 *gyr*A96 *rel*A1 *tonA*	NEB
D. fructosovorans DSM3604	Wild type strain	[18]
D. fructosovorans SM4	Δ*hndD*, Cm^r	[24]
Plasmids		
pthl-Fd-LL-C-Tag	*thlA* promoter, *CA_C0303* gene, Streptag II, *repL* gene, ColE1 origin, Amp^r	[32]
pthl-FdxB-LL-C-tag	thlA promoter, *fdxB* gene, Streptag II, *repL* gene, ColE1 origin, Amp^r	This work
pBGF4	*hyn* promoter, *hynABC* operon, Gm^r	[33, 34]
pBGF4-MCS	*hynABC* operon, MCS, Gm^r	This work
pBGF4-hndAB	pBGF4-MCS with *hndAB* inserted into NdeI and Acc65I sites	This work
pBGF4-hndABC	pBGF4-hndAB with *hndC* inserted into SpeI and Acc65I sites	This work
pBGhnd3	pBGF4-hndABC with *hndD-Streptag* inserted into AsiSI and KpnI sites	This work
pBGhnd6	pBGhnd3 with *hnd* promoter inserted into NdeI and HindIII sites to replace *hyn* promoter	This work
pTHnd	Expressing vector, T7 promoter, *hndABCD* operon, Amp^r	[25]

Abbreviations: Amp^r, ampicillin resistance; Gm^r, gentamicin resistance; Cm^r, chloramphenicol resistance, *repL* gene, gram-positive origin of replication from pIM13; *thlA* promoter, promoter of the *Clostridium acetobutylicum* ATCC 824 thiolase gene; *CA_C0303* gene, gene encoding the 2[4Fe4S]-Fd from *C. acetobutylicum*; *fdxB*, gene encoding the [4Fe4S]-Fd FdxB from *D. fructosovorans*; *hynABC* operon, operon encoding Hyn [NiFe] hydrogenase from *D. fructosovorans*; hyn promoter, promoter of *hyn* operon from *D. fructosovorans*; MCS, multiple cloning site.

Table 2: Primers used for the cloning of the *hnd* operon and the *fdxB* gene

Primer	**Sequence 5'- 3'**	**Size of amplicon (bp)**
hndAB-NdeI-dir	GACTTCCATATGCAAAACTCAACTTGCCAAGCG	956
hndAB-SpeI-Acc65I-rev	GGGGTACCATTGGACTGGCAACTAGTTTACAGGACTACCCGTTCGTA	
hndC-SpeI-dir	CGGGAGACGACGATATGGCAGCG	1508
hndC-AsiSI-Acc65I-rev	GGGGTACCATTGGACTGGCAGCGATCGCTTATTGCTTGATGATGGAGTC	
hndD-AsiSI-dir	ATGGTGCGATCGCAAGGAGGTCCGCAATGTCCATG	1800
HndD-Acc65I-Streptag-rev	TGGGGTACCTTACTTTTCGAACTGCGGGTGGGACCA	
Pr-hnd-NdeI-rev	GGAGAGGTGTTTTCATATGCC	625
Pr-hnd-HindIII-dir	GAAGCTTGCTCCGGCATGGCTCTC	
pBGF4R-MCS-dir-bis	CCGGTATGCATAGGAGGACGCATATGCGGCCGCGGA	
pBGF4R-MCS-rev-bis	ATACGTATCCTCCTGCGTATACGCCGGCGCCTGGCC	
Fd3834BglII-F	AATTAGATCTAGGAGGTTAGTTAGAATGGACACGTCCCCGCA	230
Fd3834SmaI-R	AATTCCCGGGATCCATTTCGATGCAGTCG	

2.1.1 Recombinant Hnd hydrogenase cloning

The plasmid pBGF4, carrying the [NiFe] hydrogenase *hyn* operon from *D. fructosovorans* under the control of its own promoter [33] was used to clone the four-gene *hnd* operon containing *hndA* (locus tag DesfrDRAFT_0398), *hndB* (DesfrDRAFT_0399), *hndC* (DesfrDRAFT_0400) and *hndD* (DesfrDRAFT_0401). pBGF4 is a shuttle vector of the pBM familly [34], carrying the gentamicin resistance gene.

With the aim of facilitating the cloning, a multiple cloning site (MCS) was designed and two complementary oligonucleotides were synthesized (Eurogentec) to be inserted in the pBGF4 vector downstream of the *hyn* promoter. The MCS contains SacII, NotI, NdeI, NsiI restriction enzyme sites and a Shine Dalgarno (SD) consensus sequence of ribosome binding. 0.5 µM of each oligonucleotide, pBGF4R-MCS-dir-bis and pBGF4R-MCS-rev-bis (Table 2) phosphorylated at the 5' end, were denatured 5 min in Tris-HCl 50 mM pH7.6, NaCl 200 mM at 96°C and rehybridized at room temperature overnight. Resulting double-strand DNA fragment presents cohesive ends compatible with an AgeI-digested DNA fragment and was inserted in the single AgeI restriction site of pBGF4 to give a new plasmid pBGF4-MCS. This construct was transformed in *E. coli*. Gentamicin-resistant colonies were selected, and as the fragment containing the MCS can be inserted in both orientations in the plasmid, the resulting plasmid pBGF4-MCS was verify by DNA sequencing and a plasmid with the MCS in the right orientation (SD sequence upstream the NdeI site) was selected for the following step.

Oligonucleotides hndAB-NdeI-dir and hndAB-SpeI-Acc65I-rev were used to amplify *hndA* and *hndB* genes from the pTHnd plasmid [25]. A 956-bp amplicon containing genes encoding for HndA and HndB with the addition of NdeI (upstream of *hynA*), SpeI and Acc65I (downstream of *hynB*) restriction sites was inserted into the pGEM®-T Easy vector (Promega) and then and subcloned into pBGF4-MCS using restriction sites NdeI and Acc65I to produce pBGF4-hndAB. The two oligonucleotides hndC-SpeI-dir and hndC-AsiSI-Acc65I-rev were used to amplify *hnd C* gene from the pTHnd plasmid. The purified PCR product of 1508 bp was inserted into the pGEM®-T Easy vector and the fragment containing *hndC* was cloned into pBGF4-hndAB digested with SpeI and Acc65I to give the plasmid pBGF4-hndABC. To fuse a C-terminal Strep-tag II (WSHPQFEK) to HndD, the *hndD* gene was amplified from pTHnd using the oligonucleotides hndD-AsiSI-dir and hndD-Acc65I-Streptag-Rev. A 1800-bp amplicon containing *hndD* with the addition of AsiSI and Acc65I restriction sites was inserted into the pGEM®-T Easy vector and subcloned into pBGF4-hndABC using restriction sites AsiSI and KpnI (Acc65I isoschizomer) to produce pBGhnd3.

A 625-bp PCR fragment was amplified from *D. fructosovorans* genomic DNA using primers Pr-hnd-NdeI-rev and Pr-hnd-HindIII-dir. The purified PCR fragment containing the *hnd* promoter with the addition of NdeI and HindIII restriction sites was cloned into the pGEM®-T Easy vector and then inserted in the NdeI/HindIII digested pBGhnd3 plasmid. The resulting plasmid named pBGhnd6 containing the *hnd* operon under control of its own promoter, was introduced in *D. fructosovorans* SM4 strain (Δ*hndD*) [24] by electroporation. Plasmid DNA (approximately 1 to 5 µg) was introduced into 100 µL of SM4 competent cells [34] by electroporation using 0.1 or 0.2 cm cuvettes (voltage, 1.5 kV; capacitance, 25 µF; resistance, 400 W for 0.1 cm cuvette or 700 V, 10 µF, 500 W for 0.2 cm cuvette). After electroporation, the cells were immediately suspended in 10 mL basal medium [35]. All plasmids were sequenced on both strands to ensure that no mutation had been introduced during the amplification procedure.

2.1.2 Recombinant ferredoxin cloning

We use the shuttle vector system developed by Girbal et al. in 2005 [36] to express *D. fructosovorans* Fd gene in *E. coli* MG1655 *ΔiscR::kan* strain. This plasmid was developed to overexpress genes encoding the *Clostridium acetobutylicum* [FeFe] hydrogenase and Fd [32, 36]. The *E. coli* strain MG1655 *ΔiscR* was chosen as the host strain since it is deregulated for FeS cluster assembly [37]. MG1655 *ΔiscR* is a derivative of MG1655 obtained by P1 transduction of the *ΔiscR* 777::*kan* marker (keio strain: JW2515-3).
The gene for the putative Fd FdxB (assession WP_005996647.1, locus tag DESFRDRAFT_RS18885, old locus tag DesfrDRAFT_3834) was identified in the *D. fructosovorans* genome (RefSeq : NZ_AECZ00000000.1). The coding and promoter sequence of this putative Fd was amplified from *D. fructosovorans* genomic DNA using the primers described in the Table 2, and cloned into the pthl-Fd-LL-C-Tag plasmid (Table 1) [32]. By inserting the Fd gene (in the sense orientation) between the constitutive thiolase promoter with RBS and the Strep-tag II sequence preceded by a long linker (LL: 12 amino acids "PGGSGGGSGGGS"), in this shuttle vector, we can overexpress the Strep-tagged Fd in *E. coli*. The amplified *fdxB* PCR fragment was digested with SmaI and BglII (NEB). BglII has compatible cohesive ends with BamHI, then the digested *fdxB* fragment can be ligated into the SmaI-BamHI linearised pthl-Fd-LL-C-Tag plasmid. The resulting pthl-FdxB-LL-C-tag plasmid was checked by sequencing and introduced in the *E. coli* MG1655 *ΔiscR::kan* strain by electroporation.

2.2 Culture growth conditions

D. fructosovorans SM4/pBGhnd6 cells for expression of the genes for the Strep-tagged Hnd were grown in PS2 medium (pH=6.8) containing NH_4Cl 0.43 $g.L^{-1}$, $CaSO_4,2H_2O$ 0.17 $g.L^{-1}$, NaCl 1 $g.L^{-1}$, KCl 0.5 $g.L^{-1}$, $MgSO_4,7H_2O$ 0.25 $g.L^{-1}$, sodium pyruvate 4.4 $g.L^{-1}$, KH_2PO_4 2.7 $g.L^{-1}$, $NaHCO_3$ 0.85 $g.L^{-1}$, Na_2S 0.2 $g.L^{-1}$ and 1 $mL.L^{-1}$ of a trace element solution containing $FeCl_2,4H_2O$ 7.5 $g.L^{-1}$, $CoCl_2,6H_2O$ 0.2 $g.L^{-1}$, $MnCl_2,4H_2O$ 0.1 $g.L^{-1}$, $ZnCl_2$ 70 $mg.L^{-1}$, H_3BO_3 8 $mg.L^{-1}$, $Na_2MoO_4,2H_2O$ 50 $mg.L^{-1}$, $NiCl_2,6H_2O$ 0.2 $g.L^{-1}$, $CuCl_2,2H_2O$ 12 $mg.L^{-1}$, Na_2SeO_3 17 $mg.L^{-1}$, $Na_2WO_4,2H_2O$ 34 $mg.L^{-1}$, V_2O_5 20 $mg.L^{-1}$. The strain was grown anaerobically at 37 °C in 2 L-bottles for 4 or 5 days (until the culture reaches the stationary phase). Cells were aerobically harvested by centrifugation at 8000 g for 15 min at 4 °C and the cell pellet was stored at -80°C.
The *E. coli ΔiscR*/pthl-FdxB-LL-C-tag recombinant strain for the production of FdxB was grown in anaerobic condition, in a medium containing: tryptone 11.8 $g.L^{-1}$, yeast extract 23.6 $g.L^{-1}$, K_2HPO_4 9.4 $g.L^{-1}$, KH_2PO_4 2.2 $g.L^{-1}$, glycerol 4 $mL.L^{-1}$, $FeSO_4$ 0.1 $g.L^{-1}$, L-cysteine 0.1 $g.L^{-1}$, Fe(III) citrate 0.1 $g.L^{-1}$, ammonium Fe(III) citrate 0.1 $g.L^{-1}$, in a 20 L-fermentor

(Biostat-C-30, Sartorius) maintained at 37°C. After 23 hours of growth, cells were harvested anaerobically by centrifugation, at 8000 g for 15 min at 4°C and the cell pellet was stored at -80°C.

2.3 Purification of recombinant proteins

2.3.1 Purification of the Strep-tagged Hnd hydrogenase

All steps were performed aerobically. The cell pellet was washed twice in buffer W containing Tris-HCl 100 mM pH 8.0, NaCl 150 mM and then resuspended in buffer W supplemented with protease inhibitors (SIGMAFAST™ Protease Inhibitor Cocktail Tablet, Sigma-Aldrich), DNase I (Roche) and Lysozyme (Sigma-Aldrich). Cells were disrupted by two passages through a chilled French press cell at a pressure of 100 MPa. After an ultracentrifugation at 200 000 g for 45 min at 4°C, the soluble fraction was loaded on a StrepTactin-Superflow (IBA) column (25 mL). Purification was done according to manufacturer's instructions. Strep-tagged hydrogenase was eluted by the addition of 60 mL of buffer W containing 2.5 mM desthiobiotin. Relevant fractions were pooled, dialysed to remove NaCl and desthiobiotin and concentrated (Vivaspin, molecular mass cut-off of 30 kDa; Sartorius) and separated by 12 % SDS-PAGE. Protein concentration was determined using the Bradford assay (Bio-Rad) with bovine serum albumin as the standard or by quantitative amino acid composition.

2.3.2 Purification of the Strep-tagged ferredoxin FdxB

All steps were done anaerobically in a glove box under nitrogen atmosphere. Cell pellet was resuspended in buffer W containing protease inhibitors, DNase I and Lysozyme. Cells were lysed by sonication (10 cycles of 1 min). Membranes and cell debris were removed by ultracentrifugation for 45 min at 200 000 g at 4°C. Avidin (0.1 g/L) was added to the supernatant of ultracentrifugation and after an incubation time of 1 hour, the sample was loaded on a 5mL StrepTactin-Superflow (IBA) affinity column. Purification was done according to manufacturer's instructions. Fd was eluted with 2.5 mM desthiobiotin in buffer W, dialyzed and concentrated (Vivaspin 20, molecular mass cut-off of 10 kDa; Sartorius). The purity of the Fd was checked on a 15 % SDS-PAGE and concentration of the mature Fd in oxidized form was estimated by spectrophotometry at 410 nm, corresponding to the absorption peak of iron sulfur clusters, using absorption coefficient value of 24000 M^{-1} cm^{-1}.

2.4 Enzymatic assays

All assays were performed at 30°C and under anaerobic conditions.

2.4.1 H_2-oxidizing activity

H_2-oxidizing activity measurements were performed in anaerobic quartz cuvettes, under 1 bar-pressure of H_2, in 800 µL of reaction mixture containing 100 mM Tris-HCl pH 8.0, 2 mM dithiothreitol (DTT), and 50 mM methyl viologen (Sigma Aldrich) as artificial electron acceptor. Between 10 and 200 ng of purified Hnd were added to the mixture to start the reaction and methyl viologen reduction was monitored at 604 nm (ε=13600 M^{-1}. cm^{-1}) using a UV-Vis spectrophotometer Lambda 25 (Perkin Elmer). One unit of hydrogenase activity corresponds to the uptake of 1 µmol of H_2/min.

NAD^+- and Fd-dependent H_2-oxidizing activity was assayed in anaerobic quartz cuvettes, under 1 bar of H_2, in 800 µL-mixture containing 100 mM Tris-HCl pH 8.0, 5 µM of FMN and/or 5 µM of FAD, 3 mM NAD^+ (unless otherwise specified) or 2 mM $NADP^+$ in the absence or in the presence of 20 µM of purified FdxB from *D. fructosovorans*. The reduction

of $NAD(P)^+$ was monitored at 340 nm (ε_{NADH}= 6320 M^{-1}. cm^{-1}) using a UV-Vis spectrophotometer Lambda 25 (Perkin Elmer) or $NAD(P)^+$ and FdxB reduction were followed simultaneously by recording a full spectrum every 30 s from 300 nm to 800 nm for 1h, using a Cary 60 (Varian) UV-Vis spectrophotometer. In this case, $NAD(P)^+$- and Fd-reduction rates were determined at 340 nm and 410 nm respectively using QSoas software developed by V. Fourmond [38]. The flavins were added to the mixture reaction in the presence of Hnd and FdxB and incubated in the cuvette, anaerobically, in the presence of H_2 until they were completely reduced. Then, $NAD(P)^+$ was added to start the reaction. The specific activity is given in µmol of NADH/min/mg. Absorption coefficient of oxidized FdxB was determined to be 24 000 $M^{-1}.cm^{-1}$. For the reduced ferredoxin, because of its very low redox potential, it is not possible to completely reduce the ferredoxin with usual reductant, and to determine its absorption coefficient. For $FdxB_{red}$, we used an absorption coefficient of half of the value of the determined absorption coefficient of the oxidized FdxB ($\varepsilon_{FdxBred}^{410nm}$ = 12 000 $M^{-1}.cm^{-1}$) [39, 40].

2.4.2 H_2-producing activity

H_2 evolution assays were carried out using dithionite-reduced methyl viologen (50 mM reduced with 0.1 M sodium dithionite) as electron donor, in anaerobic 8.5 mL-serum bottles containing 1 mL reaction mixture composed of Tris-HCl 0.1 M pH 8.0, at 30°C. The gas phase was 100% N_2. The reaction was started by the addition of 2.2 to 5.5 µg of purified Hnd and H_2 production was measured using gas chromatography (GC) as previously described [41]. One unit of hydrogenase activity corresponds to the production of 1 µmol of H_2/min.

2.5 Analytical techniques

2.5.1 Flavin and iron quantification

Flavin content of Hnd was determined using HPLC. The purified enzyme was denatured for 15 min at 100 °C and the denatured protein was removed by centrifugation at 14100g for 25 min. The supernatant was passed through a 0.20 µm filter before HPLC analysis using a Zorbax Eclipse Plus C18 column (5 µm, 150 x 4.6 mm, Agilent). The flavins were detected at 445 nm using a photodiode array detector (Agilent). The chromatographic separations were performed with a non-linear gradient of ammonium acetate 100 mM and methanol at a flow rate of 0.75 mL/min. An initial linear gradient of ammonium acetate from 90 to 60 % over 30 min was followed by a rapid drop to 0 % ammonium acetate (100 % methanol) (by t=35 min) and, at t=37 min, by a rapid increase to 90 % ammonium acetate in 5 min (by t=42min). Flavins were identified by comparison with the retention times of standards (FMN, FAD) and the peak area was used for quantification.

The iron content of the purified Hnd and FdxB was determined using inductively coupled plasma-optical emission spectrometry (ICP-OES) as previously described [42] and by colorimetric Iron Assay kit (Sigma-Aldrich). The concentration of protein was determined by quantitative amino acid analysis and was used to calibrate the routine Hnd concentration determination by the Bradford Assay (Bio-Rad).
The intrinsic properties of Fds (low isoelectric point, low aromatic content, small size) make their routine quantification by conventional techniques (colorimetric tests, absorption at 280 nm) difficult. Furthermore, the concentration of the mature FdxB only (containing FeS cluster) has to be considered. To determine this concentration, the absorption coefficient at 410 nm was first calculated based on iron content and the absorbance at 410 nm.

2.5.2 Dynamic light scattering

Dynamic light scattering (DLS) experiment was carried out using a Zetasizer Nano ZS (Malvern Instruments). The temperature was controlled at 25°C. Five measurements were performed; each one consisting of 10-15 runs of 10 seconds. The scattering angle was 173°. HnD was analysed at 4mg/mL in 0.1M Tris in disposable cuvettes ZEN0040. For the determination of the hydrodynamic diameter (DH), the provided software uses the Stokes-Einstein relation to obtain the intensity averaged size distribution, which requires the viscosity and refractive index values of the dispersion medium. In our case we used a viscosity of 0.9129 cP and a refractive index of 1.332 (at 25°C). To obtain the volume averaged size distribution, we use the dispersent viscosity and a standard protein refractive index of 1.450.

2.5.3 Separation by SDS-PAGE and Blue-Native gel (BN-gel) electrophoresis and in-gel hydrogenase activity detection

Proteins were separated on 15% (for FdxB) or 12% (for Hnd) polyacrylamide denaturing gels (SDS-PAGE) using a mini VE electrophoresis apparatus (Amersham Pharmacia). After migration, gels were stained with Coomassie Blue.

BN-gels were performed under aerobic condition using a mini VE electrophoresis apparatus (Amersham Pharmacia) according to the method of Schägger [43, 44] as described by Le Laz *et al*. [45]. After migration, the gel was transferred to a sealed glass bottle under anaerobic condition filled with 20 mM Tris-HCl pH 8.0 containing 2 mM methyl viologen and 2 mM 2,3,5-triphenyltetrazolium chloride for 15 min. The buffer was then flushed with H_2 and the gel was incubated in H_2-saturated buffer at room temperature until the hydrogenase activity bands were visualized in red. The gel was then stained with Coomassie Blue. The apparent molecular mass of proteins was estimated using the native molecular mass markers NativeMark (Invitrogen).

2.5.4 Protein identification by mass spectrometry

Hnd subunits were separated on a SDS-PAGE. After staining with Coomassie Blue, protein bands were cut out from gels and stored at -20°C before analysis by mass spectrometry. In-gel digestion by trypsin and MALDI-ToF-Mass Spectrometry analysis were performed as previously described by Guiral *et al*. [46], except that MS fingerprints data were searched in the non-redundant NCBI database restricted to *Desulfovibrio fructosovorans* (4 177 sequences).

2.5.5 Electron paramagnetic resonance spectroscopy (EPR)

EPR experiments were performed on a Bruker ELEXSYS E500 spectrometer equipped with an ER4102ST standard rectangular Bruker EPR resonator fitted to an Oxford Instruments ESR 900 helium flow cryostat.

Potentiometric titration of FdxB was performed as previously described [47] but in a glove-box (Jacomex). The solution contains HEPES buffer 50 mM pH 8.0, FdxB 100 µM and a mediator mix (phenosafranine 5 µM, neutral red 5 µM, methyl viologen 5 µM). Quantifications were made by using an external standard solution of 1 mM Cu-EDTA in 100 mM Tris-HCl, 10 mM EDTA at pH 8.0 transferred into a calibrated EPR tube.

Electron-bifurcation assay was performed anaerobically in a glove-box (Jacomex). The solution contains 100 mM Tris-HCl pH 8.0 saturated with 1 bar H_2, 5 mM DTT, 25 µM FAD, 5 µg of Hnd enzyme and 40 µM FdxB and was collected in 3 EPR tubes (160 µL each). The first was frozen immediately, the second incubated at room temperature for 1 hour before freezing and 2 mM of NAD^+ were added to the third which was incubated for 1 hour at room temperature before freezing. Instrument settings: 9.48 GHz, 15K, 10 mW, modulation 1.0 mT at 100 kHz.

2.5.6 UV-visible spectroscopy

UV-visible spectra were recorded in 1 cm optical length quartz cuvette closed by a septum, using a UV-Vis spectrophotometer Lambda 25 (Perkin Elmer).

2.5.7 Fourier transform infrared spectroscopy (FTIR)

The enzyme (between 200 and 400 µM in 100 mM Tris-HCl pH 8.0, 150 mM NaCl, 2.5 mM desthiobiotin, 5 µM FAD, 5 µM FMN) was injected in a gas-tight infrared transmittance cell of 82 µM path-length and analyzed with the equipment described previously [48].

3. Results

3.1 Hnd amino acid sequence analysis

The Hnd hydrogenase from *D. fructosovorans* is encoded by the four-gene *hnd* operon [25]. A Blast search [49] reveals that the same cluster of four genes is not very widespread in *Desulfovibrio* species and is only found in seven of the more than 30 sequenced *Desulfovibrio* genomes (in *D. fructosovorans*, *D. alcoholivorans*, *D. sp. FW1012B*, *D. sp. U5L*, *D. sp. DV*, *D. sp. TomC*, *D. magneticus*).

The deduced amino acid sequence of HndA, HndB, HndC and HndD proteins shows high similarity to the amino acid sequence of subunits of characterized electron-bifurcating [FeFe] hydrogenases from *A. woodii*, *T. maritima*, *M. thermoacetica*, *R. albus* and *C. autoethanogenum*. HndA shows between 30 and 45% sequence identity with HydC (or HytC) subunits of bifurcating hydrogenases. HndC, the NuoF homolog, shares between 50% and 65% sequence identity with HydB (or HytB) and HndD between 40% and 55 % sequence identity with HydA (or HytA). HndB shows 28% sequence identity with HydD subunit of the tetrameric hydrogenase from *A. woodii* (see multiple sequence alignments in Figures S1, S2, S3 and S4). Based on these sequence similarities, we assumed that Hnd is a Fd- and $NAD(P)^+$-dependent flavin-based electron-bifurcating [FeFe] hydrogenase.

3.2 Identification of genes encoding ferredoxins of *D. fructosovorans*

The electron-bifurcating activity of Hnd was measured using a purified Fd. The analysis of the draft genome sequence of *D. fructosovorans* revealed the presence of genes encoding three putative Fds. DesfrDRAFT_3400 (*fdxA*) encodes a putative Fd that shares 68% identity with the Fd II from *Desulfovibrio gigas* whose three-dimensional structure has been established [50, 51] and which can be an homodimer containing one [4Fe-4S]-cluster per monomer or an homotetramer containing one [3Fe4S]-cluster per monomer [52]. DesfrDRAFT_4133 gene (*fdxC*) is predicted to code for a 7Fe Fd containing a [3Fe4S] cluster and a [4Fe4S] cluster with 82 % sequence identity to the well-characterized Fd III of *Desulfovibrio africanus* [53-55]. The amino acid sequence deduced from DesfrDRAFT_3834 (*fdxB*) encoding the third putative Fd of *D. fructosovorans* contains 6 cysteines. It shows only low sequence identity with characterized single [4Fe4S] or [3Fe4S] cluster containing Fds from *Desulfovibrio* species (32 % with the Fd I of *D. gigas* [56], 31% with the Fd I and Fd II of *D. africanus* [53, 57], 28% with the Fd II of *Desulfovibrio vulgaris* Miyazaki [58] but shows high sequence identity with proteins deduced from genome sequence from several *Desulfovibrio* species (for example, 83% of sequence identity with deduced proteins (WP_029456869 and WP_009106863) annotated Fd from *D. alcoholivorans* and *D. sp*. U5L, and 75% identity with deduced proteins (WP_043599747 and WP_043633888=KHK03070)

from *D. magneticus* and *D. sp*. TomC). It is noteworthy that putative Fd encoding genes with high similarity to the *fdxB* gene of *D. fructosovorans* are only found in the 7 sequenced genomes of the above-mentioned *Desulfovibrio* species that also contain the *hnd* operon. The sequence of these 7 putative *Desulfovibrio* Fds contains 6 cysteine residues for the probable binding of one cubane-type cluster, distributed in two strictly conserved motifs (CCNGCGACA, CPHDCIE). This conserved sequence is different from the one found in the characterized *Desulfovibrio* Fds distributed in three motifs (CX2CX2CX3CP, C, CP) [52]. FdxB was used to test the electron-bifurcating activity of Hnd.

3.3 Cloning, production and purification of Hnd and FdxB

In order to facilitate the *in vitro* characterization of the hydrogenase, the *hnd* operon was cloned on a plasmid under the control of the native promoter and a Strep-tag II sequence was added at the 3' end of the *hndD* gene. The plasmid was then introduced in the SM4 mutant strain of *D. fructosovorans* in which *hndD* encoding the hydrogenase catalytic subunit was deleted [24]. The recombinant form of Hnd hydrogenase was aerobically-purified in one step on an affinity chromatography (Strep-Tactin resin) with a yield between 130 and 380 µg of enzyme per gram of cells. As shown in figure 2A, the elution fraction of the chromatography features four bands on SDS-PAGE stained with Coomassie blue corresponding to apparent molecular masses of 64, 52, 19, and 14 kDa, attributed to the four subunits HndD, HndC, HndA and HndB, respectively. The identification of the Hnd subunits was confirmed by mass spectrometry analysis of the four protein bands (Table S1). Blue native (BN) gel electrophoresis and diffusion light scattering (DLS) were used to determine the oligomerization state of the enzyme. DLS analysis of the purified Hnd indicates a hydrodynamic diameter of 20±1 nm that corresponds to a molecular mass of about 300 kDa (data not shown). Purified Hnd was migrated on a BN gel electrophoresis followed by in-gel detection of hydrogenase activity (Figure 2B). The activity band visible around 300 kDa was cut out from the gel and the four Hnd subunits were identified by mass spectrometry (data not shown). Taken together, these data are consistent with a homodimer of the HndABCD tetramer.

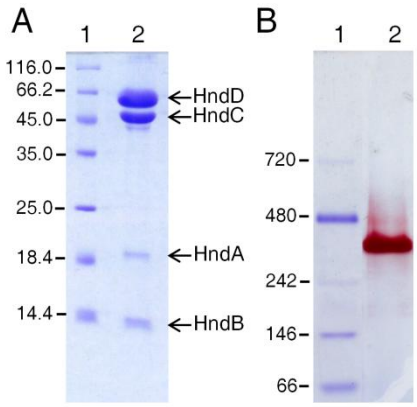

Figure 2: Denaturing and BN-gel analysis of the purified Hnd hydrogenase from *D. fructosovorans*. (A) SDS-PAGE of the purified enzyme stained with Coomassie Blue. 6µg of proteins were loaded on a 12% polyacrylamide denaturing gel. The identity of the four subunits was confirmed by MALDI-ToF mass spectrometry analysis (See Table S1). 1, Molecular mass markers (in kDa); 2, purified Hnd. (B) In-gel detection of hydrogenase activity of purified Hnd on BN-gel. 5µg of proteins were loaded on a 5-15% polyacrylamide gel. 1, Molecular mass markers (in kDa); 2, purified Hnd.

FdxB has been expressed and produced as a fusion protein with a C-terminal Strep-tag II peptide. The gene was cloned on a plasmid under the control of its own promoter and

introduced in the *E. coli* MG1655 *ΔiscR* strain deregulated for FeS cluster assembly. The Fd was anaerobically-purified using a Strep-Tactin affinity chromatography. The purification yielded between 250 and 550 µg of mature FdxB (containing the FeS cluster) per gram of cells. SDS-PAGE analysis of the purified recombinant protein showed a band with an apparent molecular mass of 15 kDa (Figure S5A) while the molecular mass of the recombinant protein predicted from the sequence is 8.7 kDa. This abnormal behavior is common in negatively charged Fds and could be due to ionic repulsion between the protein and polarized groups in the SDS gel or to unusual binding to SDS micelles [59].

3.4 Protein cofactors

3.4.1 Hnd

A bioinformatic analysis of the *hnd* operon [25] predicted a binding site for a flavin in the HndC subunit, the H-cluster binding motif in the HndD subunit and several binding sites for FeS clusters in the four different subunits. Analysis of deduced amino acid sequences of Hnd subunits allows to predict 34 or 36 iron atoms per heterotetramer (depending on the absence or the presence of a [2Fe2S] cluster in HndB subunit). Iron content of the purified enzyme was determined to be 28 ± 2 iron atoms per enzyme heterotetramer using ICP-OES and colorimetric assay. We identified and quantified the flavin by HPLC after degradation of the protein by heating and extraction of the flavins and found 0.10 ± 0.03 FMN per Hnd heterotetramer and 0.01 ± 0.005 FAD par Hnd heterotetramer. The flavin is not covalently bound to the enzyme and is probably lost during purification.

The UV-visible spectrum of the aerobically purified Hnd shows the aromatic amino acid band at 280 nm and bands between 400 and 500 nm typical of flavins and FeS clusters (Figure 3, red line). When the enzyme is reduced, either with H_2 and/or DTT, the bands between 400 and 500 nm decrease strongly (Figure 3, black line) and the difference spectrum (oxidized-reduced, Figure 3C) shows the typical feature of flavins with bands around 370 and 470 nm (FMN) or 370 and 450 nm (FAD) and the contribution of FeS clusters at 410 nm.

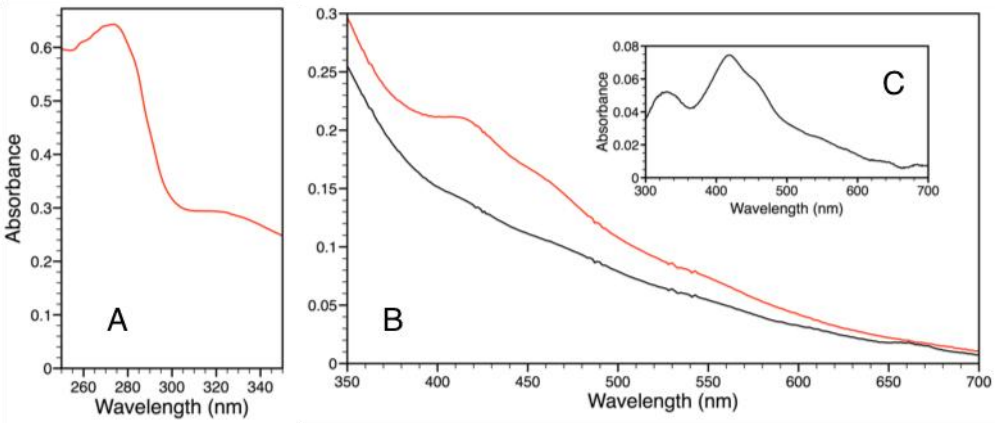

Figure 3: UV (A) and visible (B) spectrum of oxidized Hnd (0.55 g/L) in red, and of Hnd reduced with 1 bar of H_2 and DTT 5 mM in black. (C) difference spectrum (oxidized minus reduced). Optical length = 1 cm.

3.4.2 FdxB

Sequence analysis, UV-visible and EPR spectra (Figure S5B and Figure S6) show that FdxB binds a single [4Fe4S] cluster. The concentration of purified FdxB was determined by quantitative amino acid analysis and the iron content was determined by ICP-OES and colorimetric assays. From these experiments we determined that only 30% of the protein is maturated (i.e. contains its [4Fe4S]), although FdxB was produced in *E. coli* MG1655 *ΔiscR* strain overproducing the FeS cluster assembly machinery. We determined an absorption coefficient at 410 nm of 24000 M^{-1} cm^{-1} similar to that predicted or measured for a [4Fe4S]

cluster Fd (16-20 000 M^{-1} cm^{-1}) [39, 59]. The redox mid-potential of FdxB was determined by EPR titration (Figure S6) to be -450 mV/SHE.

3.5 FTIR analysis of the H-cluster of Hnd

As molecular oxygen is a strong inhibitor for most [FeFe] hydrogenases, these enzymes cannot be purified aerobically [60]. It is assumed that the inactivation of [FeFe] hydrogenases by O_2 is due to a partial degradation of the H-cluster [61-63]. By contrast, Hnd is active although it was purified under aerobic condition (see paragraph 3.6) but only after activation under reductive conditions (DTT or H_2). Dimeric hydrogenases from *Desulfovibrio* species are known to form an inactive, O_2-insensitive state of the H-cluster called H_{inact} [64] that can be detected by FTIR. The FTIR spectrum in the CO and CN^- region (1800 to 2150 cm^{-1}) of the H-cluster of the air-purified Hnd is very similar to that obtained for the H_{inact} state of hydrogenases from *D. desulfuricans* and *Clostridium beijerinckii*, with 5 bands at 2109, 2076, 2014, 1996 and 1846 cm^{-1} (Figure 4) [64, 65]. The weak bands at 2109 and 2076 cm^{-1} are attributed to the CN^- ligands, the band at 2014 cm^{-1} to the CO coordinated to the iron distal to the [4Fe4S] of the H-cluster (Fe_d), the band at 1996 cm^{-1} to the CO coordinated to the proximal iron (Fe_p) and the band at 1846 cm^{-1} is attributed to the bridging CO. This result shows that the active site of Hnd is in this H_{inact} state when the enzyme is purified under aerobic condition.

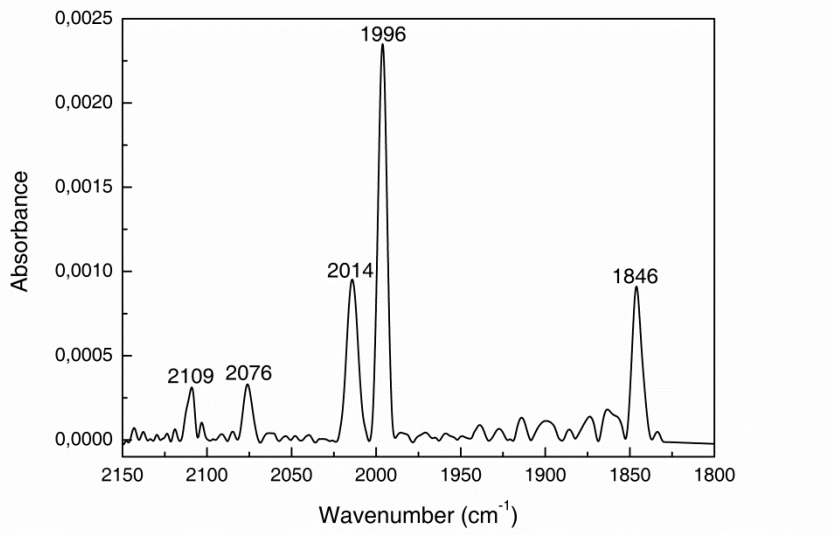

Figure 4: FTIR spectrum of aerobically purified Hnd hydrogenase in Tris 100 mM pH 8.0.

3.6 Catalytic activities with an artificial partner

Hydrogenase activity of the aerobically purified Hnd was assayed using the artificial redox partner methyl viologen, both for hydrogen production and hydrogen oxidation. We observed that, even if Hnd is active when aerobically purified, its activity is higher when the enzyme is stored under nitrogen atmosphere after purification.

The Km value for methyl viologen was determined to be 15±2 mM, both for H_2 oxidation and H_2 evolution (Figure S7). We thus used a concentration of methyl viologen of 50 mM to determine the optimal conditions for hydrogenase activity. The optimal pH and temperature were found to be pH 8 and 55°C (Figure S8), however, a DLS analysis showed enzyme degradation above 45°C (data not shown). To limit degradation, a temperature of 30°C was chosen for all catalytic activity measurements. In our experimental conditions (pH 8.0, 30°C, 50 mM methyl viologen), the specific activity of Hnd for H_2 oxidation is 2500±200 U/mg of enzyme and 155±15 U/mg of enzyme for H_2 production activity (1U= 1µmol H_2/min). It is of

note that the hydrogenase activity of the recombinant aerobically purified Hnd is in the high range of activities reported for the so far characterized electron bifurcating hydrogenases (Table S2).

3.7 Catalytic activities with physiological partners

As we propose that Hnd interacts with $NAD(P)^+$ and a Fd to catalyze a bifurcating (or confurcating) reaction in the physiological context, we tested the capacity of this enzyme to reduce these compounds under 1 bar of H_2. First, the purified Hnd does not reduce $NADP^+$ under any condition tested whereas it is able to reduce NAD^+ (Figure S9) showing that the hydrogenase is NAD- rather than NADP-specific. This result was very surprising since Hnd was previously described as an NADP-reducing enzyme [25, 26].
Electron bifurcating hydrogenases reduce or oxidize simultaneously two redox partners, NAD and a Fd. The reduction of Fd by Hnd was followed by EPR spectroscopy (Figure 5). We observed the reduction of FdxB by the enzyme only in the presence of NAD^+ in the assay mixture with the appearance of a signal typical of a reduced [4Fe4S] cluster with g-values of 2.08, 1.93 and 1.89. No Fd reduction is visible when NAD^+ is absent indicating that the presence of the two partners is essential for the Fd reduction.

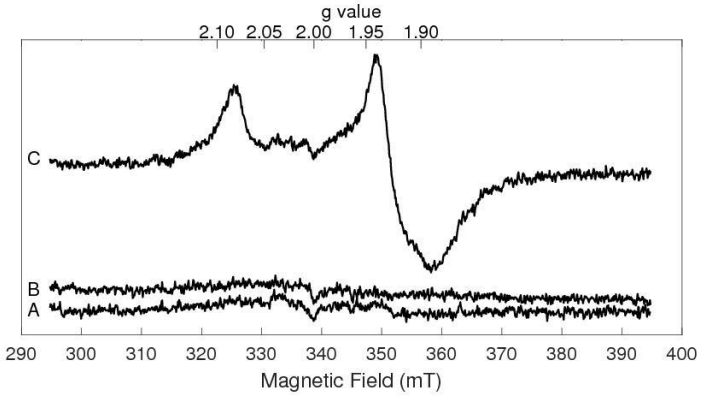

Figure 5: FdxB reduction by Hnd monitored by EPR spectroscopy. The EPR tubes were prepared under strictly anaerobic condition. In the absence of NAD^+ at t=0 min (A) and after 1h of incubation (B), and in the presence of 2 mM NAD^+ after 1h of incubation (C). The assay mixture, under 1 bar of H_2, contained 0.1 M Tris pH 8.0, 5 mM DTT, 25 µM FAD, 27 µM FdxB, and 5 µg of Hnd. Instrument settings: 9.48 GHz, 15K, 10 mW, modulation 1.0 mT at 100 kHz.

On the other hand, the reduction of NAD^+ was followed by UV-visible spectrophotometry in the absence or in the presence of FdxB (Figure 6). The NAD^+-reduction activity is strongly stimulated by the addition of Fd. Surprisingly, however Hnd is also able to reduce NAD^+ in the absence of the Fd, albeit with a 10 to 20-fold lower activity.

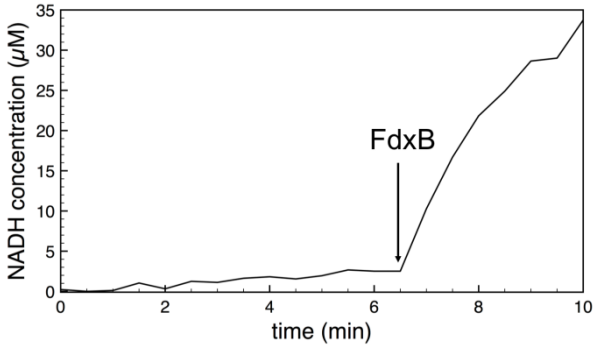

Figure 6: NAD^+ reduction by Hnd monitored at 340 nm. The assay mixture in anaerobic cuvette under 1 bar of H_2 contained 0.1 M Tris pH 8.0, 2.5 mM DTT, 5 µM FMN, 5 µM FAD, 2 µg of Hnd and 6 mM NAD^+. After t= 6.5 min, 20 µM of FdxB was added.

These results demonstrate that Hnd is a Fd- and NAD^+-dependent hydrogenase. The reduction of both NAD^+ and FdxB by the enzyme was then followed simultaneously by recording a full visible spectrum every 30s (Figure 7A) to have a full overview of the reduction process. As previously described for electron-bifurcating hydrogenases [6, 7, 9], we found that the presence of flavins in the assay mixture is required to detect Hnd activity. The catalytic activity of Hnd was similar in the presence of either FMN or FAD at the same concentration or in the presence of the same concentration of a mixture of both flavins. A mixture of 5 µM of FMN and 5 µM of FAD was used. We observed that additional flavins are reduced by the enzyme under H_2, in the absence of the two electron acceptors NAD^+ and FdxB, resulting in a decrease of the absorbance in the 410 nm region. As reduction of exogenous flavins could interfere with the monitoring of the Fd reduction at the same wavelength, we allowed Hnd to reduce the additional flavins in the presence of H_2 before starting the reaction by addition of NAD^+ and FdxB. This method allows us to make sure that the decrease in absorbance at 410 nm is only due to Fd reduction. From the full spectra recorded as a function of time (Figure 7A), absorbance values at 340 nm and 410 nm were extracted allowing the determination of the reduction kinetics of NAD^+ and FdxB respectively (Figures 7B and S10).

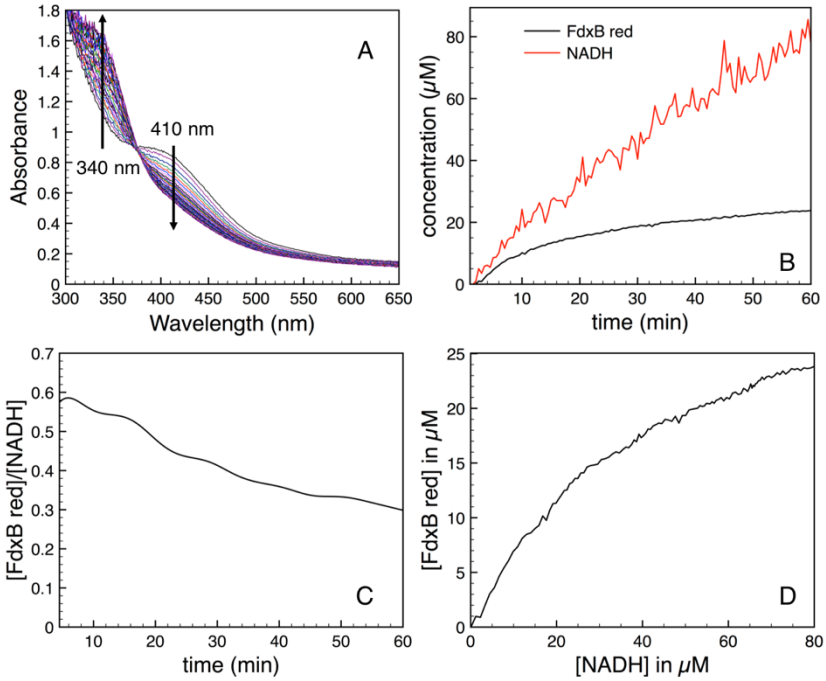

Figure 7: Electron-bifurcating activity of Hnd. (A) Spectra evolution during H_2 oxidation. For the sake of clarity, only spectra recorded every 2 minutes are shown (from t=0 to t=60 min). (B) kinetics of NAD^+ (in red) and FdxB (in black) reduction from experiment shown in panel (A) monitored at 340 nm and 410 nm respectively. (C) Ratio $[FdxB_{red}]/[NADH]$ as function of time. (D) Stoichiometry of Fd and NAD^+ reduction. Concentration of reduced FdxB as a function of the concentration of NADH. The assay mixture, in anaerobic cuvette under 1 bar of H_2, contained 0.1 M Tris pH 8.0, 2.5 mM DTT, 5 µM FMN, 5 µM FAD, 20 µM FdxB, 900 ng of Hnd. After the complete reduction of flavins, the reaction was started with the addition of 3 mM NAD^+. The [NADH] data of panel (C) and (D) were smoothed using "fft-filter" in Qsoas softwave [38].

Figures 7 A and B show the simultaneous reduction of NAD^+ and FdxB with H_2 by Hnd. The specific activity of Hnd was calculated from the initial rate of NAD^+ reduction and was found to be 10±1 µmol NADH produced/min/mg of enzyme. This activity decreased over time to stabilize around 1.5 µmol/min/mg after enzyme storage for 1 day at 4°C or few months in liquid nitrogen. The Hnd enzyme catalyzes the coupled reduction of NAD^+ and FdxB, as is the case for the characterized electron-bifurcating hydrogenases. However, the fact that, FdxB

reduction reaches a plateau (at t~15 min in Figure 7B) to a value corresponding to the initial concentration of FdxB, while NAD^+ reduction persists, was unexpected. The ratio $[FdxB_{red}]/[NADH]$ (Figure 7C) and the stoichiometry (Figure 7D) vary over the reaction with a decreasing amount of FdxB reduced per NADH produced. The stoichiometry and its evolution are not that expected for a typical electron bifurcating reaction involving NAD^+ and a Fd containing a single FeS cluster able to transfer only one electron at a time. Moreover, the initial stoichiometry of the reaction does not depend on the NAD^+ concentration used in the assay and is 0.68 ± 0.13 reduced FdxB per NADH (Figure S11). The Michaelis constant of the enzyme for NAD^+ was determined to be 0.35±0.10 mM (Figure S11).

4. Discussion

We used the homologous expression system of *D. fructosovorans* to produce a Strep-tagged form of the Hnd hydrogenase. The recombinant enzyme produced is stable and is purified as a dimer of a heterotetrameric complex HndABCD with an apparent molecular mass around 300 kDa. The moderate production of the enzyme by this system allows the natural hydrogenase maturation machinery produced from chromosomal genes to maturate Hnd, as attested by the iron content of the purified enzyme. In order to determine if Hnd is an electron-bifurcating enzyme, the gene encoding one of the three Fd from *D. fructosovorans* was overexpressed in *E. coli* and a recombinant form of the FdxB Fd was purified and shown to contain a low-potential [4Fe4S] cluster (-450 mV).

The methyl viologen reducing-activity of Hnd is in the higher range of the activity of other electron-bifurcating hydrogenases (2500 U/mg for Hnd versus 181 U/mg for hydrogenase from *M. thermoacetica*, 760 U/mg for hydrogenase from *A. woodii*, 70 U/mg for hydrogenase from *T. maritima* and 18000 for hydrogenase from *C. autoethanogenum*) [6-9]. The electron-bifurcating hydrogenase activity of Hnd with NAD^+ and FdxB as redox partners, under H_2, is 10 U/mg of enzyme in the best conditions and is in the range of that obtained with the characterized electron-bifurcating hydrogenases (between 3 and 60 U/mg of enzyme) [7-10] (Table S2).

Although Hnd hydrogenase was purified under aerobic conditions, it is fully active after reactivation under reductive conditions (incubation in the presence of DTT and/or H_2). This property is due to the formation of the H_{inact} state of the catalytic site, as shown by FTIR spectroscopy. This inactive state, protecting the enzyme against inhibition by O_2, is characteristic of the *Desulfovibrio* species [FeFe] hydrogenases [66] and was observed only in another bacterial species, *Clostridium beijerinckii* [65]. Hnd is the first example of electron-bifurcating hydrogenases able to form the H_{inact} state of the H-cluster.

We demonstrated that Hnd is a NAD-specific hydrogenase and not an NADP-specific enzyme. This result is in contradiction with previous studies [25, 26] in which an H_2-dependent $NADP^+$-reducing activity was measured on cell extracts of *D. fructosovorans*. This activity was assigned to Hnd because it was completely abolished in *hndC* or *hndD* deletion mutant strains. More recently, we identified an operon encoding a putative trimeric electron-bifurcating hydrogenase in the draft genome of *D. fructosovorans* that may be responsible for the $NADP^+$-reducing activity detected initially in the WT strain. In the *hnd* deletion mutant strains, the expression of the putative trimeric hydrogenase may be strongly down-regulated and not detectable anymore. Cloning of the genes encoding this putative electron-bifurcating hydrogenase is ongoing in our lab in order to characterize the enzyme as well as the study of its expression in different mutant strains of *D. fructosovorans*.

Electron bifurcating hydrogenases are described to couple exergonic reduction of NAD^+ to endergonic reduction of Fd [6, 7, 9]. In our experimental conditions (pH 8.0, 1 bar H_2), the Nernst potential of the H^+/H_2 couple is -480 mV/SHE. The apparent standard potential at pH 8.0 is E°'=-350 mV/SHE for the NAD^+/NADH couple and the measured potential of the $FdxB_{ox}/FdxB_{red}$ couple is -450 mV/SHE (Figure S6). Redox potentials of both electron acceptors (NAD^+ and FdxB) are thus higher than that of the donor (H_2). It is of note that in the literature, the experimental conditions were not always taken into account in calculating the effective redox potential of the NAD^+/NADH and H^+/H_2 couples (for example, the H^+/H_2 redox potential was given as -414 mV instead of -481 mV in Schuchmann and Müller (2012) [7] and -450 mV in Wang et al. (2013) [9]. Furthermore, the *C. pasteurianum* Fd is usually used as redox partner in electron bifurcation experiments and its proposed potential varies between -500 mV [7] and -400 mV [9]. The high value is suggested by experimental evidences (-412 mV by EPR redox titration or -400 mV by electrochemistry) [67, 68], while the low value was stipulated *ad hoc*. If these potentials are considered, reduction of the two acceptors, NAD^+ and Fd, is exergonic, as it is the case for Hnd hydrogenase. To better explain electron bifurcation, which strictly couples the two exergonic and endergonic reductions, redox potentials of cofactors that are part of electron transfer chain in the hydrogenase must be considered. Moreover, we found that Hnd is able to reduce NAD^+ in the absence of Fd as was also observed for *A. woodii* bifurcating hydrogenase [7]. From a thermodynamic point of view, it should therefore be possible to reduce NAD^+ by H_2, although a mechanistic rationalization for the ensemble of the observed redox reactions still needs to be elaborated.

Concerning the flavin cofactors, both FAD and FMN were detected by HPLC but at low population levels (10 % of FMN and less than 1% of FAD). This is explained by the absence of strong interaction between the flavin and the enzyme, leading to the loss of the flavin during the purification process as in most other flavoproteins studied to date. Furthermore, we found that the presence of flavin in the activity assay is essential to detect the electron bifurcating activity of Hnd and that the nature of the flavin added (FMN or FAD) does not influence the value of this activity. The bifurcating activity of the Hyd enzymes from *M. thermoacetica* and *T. maritima* is stimulated by FMN and also by FAD but to a lesser extent [6, 9]. These results could be explained by the presence in Hnd of either 2 flavin binding sites or only one flavin binding site that can accommodate the 2 types of flavins, FMN and FAD. We favor the former hypothesis because it is in agreement with the fact that the enzyme must contain two 2-electron sites, one needed for the NAD^+/NADH conversion and the other for the electron bifurcating reaction (Figure 8) as this was already proposed by Buckel and Thauer [13, 14]. The flavin-site involved in NAD^+ reduction is probably the one predicted from the HndC sequence, close to the NAD^+ pocket [25]. HndC is sequence-related to NuoF, the FMN-harboring subunit of the NADH dehydrogenase complex of *E. coli*. The flavin in this site accepts electrons one by one probably from one of the FeS cluster of HndC and thus must present a stable semi-oxidized form. A second 2-electron site must be present in the enzyme with "crossed" redox transitions [69] to perform electron-bifurcation. This site of bifurcating flavin, although not predicted by subunit sequences, is likely located in HndC or at the interface between subunits. Peters et al. (2018) [70] recently proposed that the electron bifurcating site could be the H-cluster of electron-bifurcating hydrogenases. This hypothesis seems unlikely to us for structural reasons. By analogy with the “standard” CpI [FeFe] hydrogenase from *C. pasteurianum*, only one electron transfer chain to or from the buried active site would be present in bifurcating hydrogenases [71].

The electron-bifurcating hydrogenases from *A. woodii* and *M. thermoacetica* reduce one NAD^+ per *C. pasteurianum* Fd [7, 9] (containing 2 isopotential [4Fe4S]-clusters) [67]. For Hnd, the ratio of $[Fd_{red}]$/[NADH] varies during the reaction and much more NADH is produced compared to the amount of Fd present in the activity assay while FdxB is a single FeS cluster-Fd (Figure 7). Moreover, in figure 7B, the NAD^+ reduction kinetics remains constant even after FdxB reduction is almost complete. These observations could be explained by a model in which FdxB is recycled (Figure 8). In this model, FdxB and NAD^+ are reduced simultaneously by Hnd by an electron bifurcating reaction. The reduced Fd would then be reoxidized by one of the two distal FeS clusters of HndD. In monomeric clostridial [FeFe] hydrogenases, the electron transfer chain presents an unusual Y shape, with two surface-exposed distal FeS clusters named FS2 and FS4C, the role of which is not yet explained [32]. Since the amino acid sequence of the hydrogenase catalytic subunit of Hnd is very similar to that of monomeric clostridial hydrogenases, we can assume that this Y-shaped electron transfer chain is also present in Hnd. The oxidized Fd produced by this cycle can be reduced again by the electron- bifurcating reaction. This model would explain the presence of this Y-shaped chain in bifurcating hydrogenases which could be an ancestor of the monomeric clostridial hydrogenases. This hypothesis will be investigated in future studies.

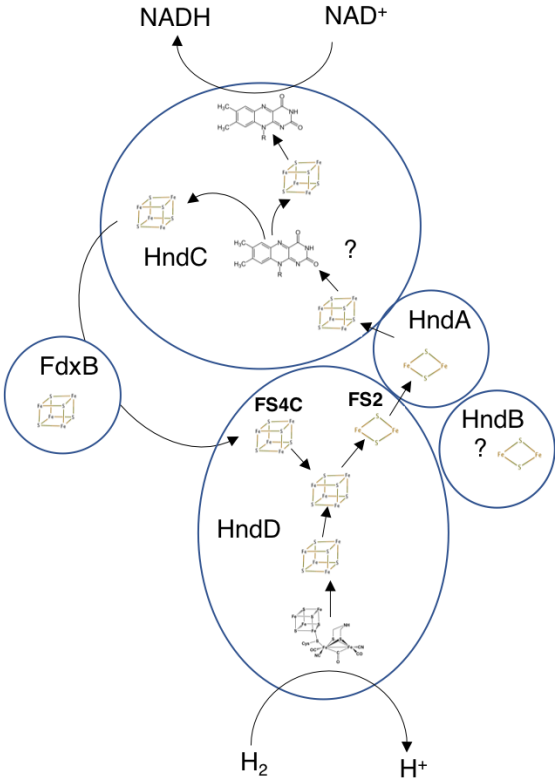

Figure 8: Proposed model of the electron-bifurcating hydrogenase Hnd from *D. fructosovorans*, in which the Fd is recycled. The composition of cofactors is based on amino acid sequence analysis. The presence of a [2Fe2S] cluster in HndB is uncertain because the cluster binding motif is not conserved [28].The subunit arrangement is arbitrary except for HndA which has been shown to interact with HndD [28]. The Y-shaped electron transfer chain in HndD is based on the analogy with [FeFe] clostridial hydrogenases [31, 32]. The choice of the position of distal FeS clusters (FS2 and FS4C) of HndD is arbitrary.

Acknowledgments

The authors thank I. Meynial-Salles and P. Soucaille for kindly providing the plasmid pthl-Fd-LL-C-Tag, D. Byrne from the protein expression facility of the Mediterranean Institute of Microbiology (IMM, Marseille) for DLS experiments, J.-P. Andrieu of IBS (Grenoble) for

quantitative amino acid analysis, A. Zellat of BIP (UMR7283 CNRS/AMU) for ICP-OES experiments. The authors thank the national french EPR network (RENARD, IR3443, http://renard.univ-lille1.fr). S. Lignon (deceased), P. Mansuelle and R. Lebrun from the Proteomic Platform of IMM, CNRS FR3479, Marseille Protéomique -IBiSA and -Aix Marseille Univ labeled, are acknowledged for mass spectrometry analyses. We thank V. Fourmond for data analysis QSoas software script, W. Nitschke and M. Guiral for helpful discussions and for critical reading of the manuscript. A.L.D. and G.G-M. thank MINECO/FEDER for project funding (CTQ2015-71590-R) and a predoctoral contract (BES-2016-078815) respectively.

References:

[1] P.M. Vignais, B. Billoud, J. Meyer, Classification and phylogeny of hydrogenases, FEMS Microbiol Rev, 25 (2001) 455-501.
[2] P.M. Vignais, B. Billoud, Occurrence, classification, and biological function of hydrogenases: an overview, Chem Rev, 107 (2007) 4206-4272.
[3] J.W. Peters, G.J. Schut, E.S. Boyd, D.W. Mulder, E.M. Shepard, J.B. Broderick, P.W. King, M.W. Adams, [FeFe]- and [NiFe]-hydrogenase diversity, mechanism, and maturation, Biochim Biophys Acta, 1853 (2015) 1350-1369.
[4] J.C. Fontecilla-Camps, A. Volbeda, C. Cavazza, Y. Nicolet, Structure/Function Relationships of [NiFe]- and [FeFe]-Hydrogenases, Chem Rev, 107 (2007) 4273-4303.
[5] C. Greening, A. Biswas, C.R. Carere, C.J. Jackson, M.C. Taylor, M.B. Stott, G.M. Cook, S.E. Morales, Genomic and metagenomic surveys of hydrogenase distribution indicate H_2 is a widely utilised energy source for microbial growth and survival, ISME J, 10 (2016) 761-777.
[6] G.J. Schut, M.W. Adams, The iron-hydrogenase of *Thermotoga maritima* utilizes ferredoxin and NADH synergistically: a new perspective on anaerobic hydrogen production, J Bacteriol, 191 (2009) 4451-4457.
[7] K. Schuchmann, V. Müller, A bacterial electron-bifurcating hydrogenase, J Biol Chem, 287 (2012) 31165-31171.
[8] S. Wang, H. Huang, J. Kahnt, A.P. Mueller, M. Kopke, R.K. Thauer, NADP-specific electron-bifurcating [FeFe]-hydrogenase in a functional complex with formate dehydrogenase in *Clostridium autoethanogenum* grown on CO, J Bacteriol, 195 (2013) 4373-4386.
[9] S. Wang, H. Huang, J. Kahnt, R.K. Thauer, A reversible electron-bifurcating ferredoxin- and NAD-dependent [FeFe]-hydrogenase (HydABC) in *Moorella thermoacetica*, J Bacteriol, 195 (2013) 1267-1275.
[10] Y. Zheng, J. Kahnt, I.H. Kwon, R.I. Mackie, R.K. Thauer, Hydrogen formation and its regulation in *Ruminococcus albus*: involvement of an electron-bifurcating [FeFe]-hydrogenase, of a non-electron-bifurcating [FeFe]-hydrogenase, and of a putative hydrogen-sensing [FeFe]-hydrogenase, J Bacteriol, 196 (2014) 3840-3852.
[11] W. Buckel, R.K. Thauer, Energy conservation via electron bifurcating ferredoxin reduction and proton/Na(+) translocating ferredoxin oxidation, Biochim Biophys Acta, 1827 (2013) 94-113.
[12] F. Li, J. Hinderberger, H. Seedorf, J. Zhang, W. Buckel, R.K. Thauer, Coupled ferredoxin and crotonyl coenzyme A (CoA) reduction with NADH catalyzed by the butyryl-CoA dehydrogenase/Etf complex from *Clostridium kluyveri*, J Bacteriol, 190 (2008) 843-850.
[13] W. Buckel, R.K. Thauer, Flavin-Based Electron Bifurcation, Ferredoxin, Flavodoxin, and Anaerobic Respiration With Protons (Ech) or NAD(+) (Rnf) as Electron Acceptors: A Historical Review, Front Microbiol, 9 (2018) 401.
[14] W. Buckel, R.K. Thauer, Flavin-Based Electron Bifurcation, A New Mechanism of Biological Energy Coupling, Chem Rev, (2018).

[15] S. Poudel, M. Tokmina-Lukaszewska, D.R. Colman, M. Refai, G.J. Schut, P.W. King, P.C. Maness, M.W. Adams, J.W. Peters, B. Bothner, E.S. Boyd, Unification of [FeFe]-hydrogenases into three structural and functional groups, Biochim Biophys Acta, 1860 (2016) 1910-1921.
[16] W. Badziong, R.K. Thauer, J.G. Zeikus, Isolation and characterization of *Desulfovibrio* growing on hydrogen plus sulfate as the sole energy source, Arch Microbiol, 116 (1978) 41-49.
[17] A.T. Brandis, R. K., Growth of *Desulfovibrio* species on hydrogen and sulphate as sole energy source, Journal of General Microbiology, 126 (1981) 249-252.
[18] B. Ollivier, R. Cord-Ruwisch, E.C. Hatchikian, J.L. Garcia, Characterization of *Desulfovibrio fructosovorans* sp. nov., Arch Microbiol, 149 (1988) 447-450.
[19] M. Rousset, Z. Dermoun, C.E. Hatchikian, J.P. Belaich, Cloning and sequencing of the locus encoding the large and small subunit genes of the periplasmic [NiFe]hydrogenase from *Desulfovibrio fructosovorans*, Gene, 94 (1990) 95-101.
[20] C.E. Hatchikian, A.S. Traore, V.M. Fernandez, R. Cammack, Characterization of the nickel-iron periplasmic hydrogenase from *Desulfovibrio fructosovorans*, Eur J Biochem, 187 (1990) 635-643.
[21] P.P. Liebgott, A.L. de Lacey, B. Burlat, L. Cournac, P. Richaud, M. Brugna, V.M. Fernandez, B. Guigliarelli, M. Rousset, C. Leger, S. Dementin, Original design of an oxygen-tolerant [NiFe] hydrogenase: major effect of a valine-to-cysteine mutation near the active site, J Am Chem Soc, 133 (2011) 986-997.
[22] A. Abou Hamdan, B. Burlat, O. Gutierrez-Sanz, P.P. Liebgott, C. Baffert, A.L. De Lacey, M. Rousset, B. Guigliarelli, C. Leger, S. Dementin, O_2-independent formation of the inactive states of NiFe hydrogenase, Nat Chem Biol, 9 (2013) 15-17.
[23] L. Casalot, C.E. Hatchikian, N. Forget, P. de Philip, Z. Dermoun, J.P. Belaich, M. Rousset, Molecular study and partial characterization of iron-only hydrogenase in *Desulfovibrio fructosovorans*, Anaerobe, 4 (1998) 45-55.
[24] S. Malki, G. De Luca, M.L. Fardeau, M. Rousset, J.P. Belaich, Z. Dermoun, Physiological characteristics and growth behavior of single and double hydrogenase mutants of *Desulfovibrio fructosovorans*, Arch Microbiol, 167 (1997) 38-45.
[25] S. Malki, I. Saimmaime, G. De Luca, M. Rousset, Z. Dermoun, J.P. Belaich, Characterization of an operon encoding an NADP-reducing hydrogenase in *Desulfovibrio fructosovorans*, J Bacteriol, 177 (1995) 2628-2636.
[26] G. de Luca, P. de Philip, M. Rousset, J.P. Belaich, Z. Dermoun, The NADP-reducing hydrogenase of *Desulfovibrio fructosovorans*: evidence for a native complex with hydrogen-dependent methyl-viologen-reducing activity, Biochem Biophys Res Commun, 248 (1998) 591-596.
[27] G. de Luca, M. Asso, J.P. Belaich, Z. Dermoun, Purification and characterization of the HndA subunit of NADP-reducing hydrogenase from *Desulfovibrio fructosovorans* overproduced in *Escherichia coli*, Biochemistry, 37 (1998) 2660-2665.
[28] Z. Dermoun, G. De Luca, M. Asso, P. Bertrand, F. Guerlesquin, B. Guigliarelli, The NADP-reducing hydrogenase from *Desulfovibrio fructosovorans*: functional interaction between the C-terminal region of HndA and the N-terminal region of HndD subunits, Biochim Biophys Acta, 1556 (2002) 217-225.
[29] M. Nouailler, X. Morelli, O. Bornet, B. Chetrit, Z. Dermoun, F. Guerlesquin, Solution structure of HndAc: a thioredoxin-like domain involved in the NADP-reducing hydrogenase complex, Protein Sci, 15 (2006) 1369-1378.
[30] J. Meyer, J. Gagnon, Primary structure of hydrogenase I from *Clostridium pasteurianum*, Biochemistry, 30 (1991) 9697-9704.

[31] J.W. Peters, W.N. Lanzilotta, B.J. Lemon, L.C. Seefeldt, X-ray crystal structure of the Fe-only hydrogenase (CpI) from *Clostridium pasteurianum* to 1.8 angstrom resolution, Science, 282 (1998) 1853-1858.
[32] C. Gauquelin, C. Baffert, P. Richaud, E. Kamionka, E. Etienne, D. Guieysse, L. Girbal, V. Fourmond, I. Andre, B. Guigliarelli, C. Leger, P. Soucaille, I. Meynial-Salles, Roles of the F-domain in [FeFe] hydrogenase, Biochim Biophys Acta, 1859 (2018) 69-77.
[33] S. Dementin, B. Burlat, A.L. De Lacey, A. Pardo, G. Adryanczyk-Perrier, B. Guigliarelli, V.M. Fernandez, M. Rousset, A glutamate is the essential proton transfer gate during the catalytic cycle of the [NiFe] hydrogenase, J Biol Chem, 279 (2004) 10508-10513.
[34] M. Rousset, L. Casalot, B.J. Rapp-Giles, Z. Dermoun, P. de Philip, J.P. Belaich, J.D. Wall, New shuttle vectors for the introduction of cloned DNA in Desulfovibrio, Plasmid, 39 (1998) 114-122.
[35] P.P. Liebgott, F. Leroux, B. Burlat, S. Dementin, C. Baffert, T. Lautier, V. Fourmond, P. Ceccaldi, C. Cavazza, I. Meynial-Salles, P. Soucaille, J.C. Fontecilla-Camps, B. Guigliarelli, P. Bertrand, M. Rousset, C. Leger, Relating diffusion along the substrate tunnel and oxygen sensitivity in hydrogenase, Nat Chem Biol, 6 (2010) 63-70.
[36] L. Girbal, G. von Abendroth, M. Winkler, P.M. Benton, I. Meynial-Salles, C. Croux, J.W. Peters, T. Happe, P. Soucaille, Homologous and heterologous overexpression in *Clostridium acetobutylicum* and characterization of purified clostridial and algal Fe-only hydrogenases with high specific activities, Appl Environ Microbiol, 71 (2005) 2777-2781.
[37] C.J. Schwartz, J.L. Giel, T. Patschkowski, C. Luther, F.J. Ruzicka, H. Beinert, P.J. Kiley, IscR, an Fe-S cluster-containing transcription factor, represses expression of Escherichia coli genes encoding Fe-S cluster assembly proteins, Proc Natl Acad Sci U S A, 98 (2001) 14895-14900.
[38] V. Fourmond, QSoas: A Versatile Software for Data Analysis, Anal Chem, 88 (2016) 5050-5052.
[39] W.V. Sweeney, J.C. Rabinowitz, Proteins containing 4Fe-4S clusters: an overview, Annu Rev Biochem, 49 (1980) 139-161.
[40] L. Pieulle, B. Guigliarelli, M. Asso, F. Dole, A. Bernadac, E.C. Hatchikian, Isolation and characterization of the pyruvate-ferredoxin oxidoreductase from the sulfate-reducing bacterium *Desulfovibrio africanus*, Biochim Biophys Acta, 1250 (1995) 49-59.
[41] L. Avilan, B. Roumezi, V. Risoul, C.S. Bernard, A. Kpebe, M. Belhadjhassine, M. Rousset, M. Brugna, A. Latifi, Phototrophic hydrogen production from a clostridial [FeFe] hydrogenase expressed in the heterocysts of the cyanobacterium *Nostoc PCC 7120*, Appl Microbiol Biotechnol, (2018).
[42] J. Hadj-Saïd, M.E. Pandelia, C. Leger, V. Fourmond, S. Dementin, The Carbon Monoxide Dehydrogenase from *Desulfovibrio vulgaris*, Biochim Biophys Acta, 1847 (2015) 1574-1583.
[43] H. Schägger, G. von Jagow, Blue native electrophoresis for isolation of membrane protein complexes in enzymatically active form, Anal Biochem, 199 (1991) 223-231.
[44] H. Schägger, W.A. Cramer, G. von Jagow, Analysis of molecular masses and oligomeric states of protein complexes by blue native electrophoresis and isolation of membrane protein complexes by two-dimensional native electrophoresis, Anal Biochem, 217 (1994) 220-230.
[45] S. Le Laz, A. Kpebe, M. Bauzan, S. Lignon, M. Rousset, M. Brugna, A biochemical approach to study the role of the terminal oxidases in aerobic respiration in *Shewanella oneidensis* MR-1, PLoS One, 9 (2014) e86343.
[46] M. Guiral, L. Prunetti, S. Lignon, R. Lebrun, D. Moinier, M.T. Giudici-Orticonit, New insights into the respiratory chains of the chemolithoautotrophic and hyperthermophilic bacterium *Aquifex aeolicus*, J Proteome Res, 8 (2009) 1717-1730.

[47] S. Dementin, B. Burlat, V. Fourmond, F. Leroux, P.P. Liebgott, A. Abou Hamdan, C. Leger, M. Rousset, B. Guigliarelli, P. Bertrand, Rates of intra- and intermolecular electron transfers in hydrogenase deduced from steady-state activity measurements, J Am Chem Soc, 133 (2011) 10211-10221.
[48] C. Di Bari, N. Mano, S. Shleev, M. Pita, A.L. De Lacey, Halides inhibition of multicopper oxidases studied by FTIR spectroelectrochemistry using azide as an active infrared probe, J Biol Inorg Chem, 22 (2017) 1179-1186.
[49] M. Johnson, I. Zaretskaya, Y. Raytselis, Y. Merezhuk, S. McGinnis, T.L. Madden, NCBI BLAST: a better web interface, Nucleic Acids Res, 36 (2008) W5-9.
[50] C.R. Kissinger, L.C. Sieker, E.T. Adman, L.H. Jensen, Refined crystal structure of ferredoxin II from *Desulfovibrio gigas* at 1.7 A, J Mol Biol, 219 (1991) 693-715.
[51] B.J. Goodfellow, A.L. Macedo, P. Rodrigues, I. Moura, V. Wray, J.J. Moura, The solution structure of a [3Fe-4S] ferredoxin: oxidised ferredoxin II from *Desulfovibrio gigas*, J Biol Inorg Chem, 4 (1999) 421-430.
[52] J.J. Moura, A.L. Macedo, P.N. Palma, Ferredoxins, Methods Enzymol, 243 (1994) 165-188.
[53] L. Pieulle, M.H. Charon, P. Bianco, J. Bonicel, Y. Petillot, E.C. Hatchikian, Structural and kinetic studies of the pyruvate-ferredoxin oxidoreductase/ferredoxin complex from *Desulfovibrio africanus*, Eur J Biochem, 264 (1999) 500-508.
[54] F.A. Armstrong, S.J. George, R. Cammack, E.C. Hatchikian, A.J. Thomson, Electrochemical and spectroscopic characterization of the 7Fe form of ferredoxin III from *Desulfovibrio africanus*, Biochem J, 264 (1989) 265-273.
[55] S.J. George, F.A. Armstrong, E.C. Hatchikian, A.J. Thomson, Electrochemical and spectroscopic characterization of the conversion of the 7Fe into the 8Fe form of ferredoxin III from *Desulfovibrio africanus*. Identification of a [4Fe-4S] cluster with one non-cysteine ligand, Biochem J, 264 (1989) 275-284.
[56] M. Bruschi, P. Couchoud, Amino acid sequence of *Desulfovibrio gigas* ferredoxin: revisions, Biochem Biophys Res Commun, 91 (1979) 623-628.
[57] E.C. Hatchikian, R. Cammack, D.S. Patil, A.E. Robinson, A.J.M. Richards, S. George, A.J. Thomson, Spectroscopic characterization of ferredoxins I and II from *Desulfovibrio africanus*, Biochim Biophys Acta, 784 (1984) 40-47.
[58] N. Okawara, M. Ogata, T. Yagi, S. Wakabayashi, H. Matsubara, Characterization and complete amino acid sequence of ferredoxin II from *Desulfovibrio vulgaris* Miyazaki, Biochimie, 70 (1988) 1815-1820.
[59] B. Darimont, R. Sterner, Sequence, assembly and evolution of a primordial ferredoxin from *Thermotoga maritima*, EMBO J, 13 (1994) 1772-1781.
[60] C. Orain, L. Saujet, C. Gauquelin, P. Soucaille, I. Meynial-Salles, C. Baffert, V. Fourmond, H. Bottin, C. Leger, Electrochemical Measurements of the Kinetics of Inhibition of Two FeFe Hydrogenases by O_2 Demonstrate That the Reaction Is Partly Reversible, J Am Chem Soc, 137 (2015) 12580-12587.
[61] C. Lambertz, N. Leidel, K.G. Havelius, J. Noth, P. Chernev, M. Winkler, T. Happe, M. Haumann, O_2 reactions at the six-iron active site (H-cluster) in [FeFe]-hydrogenase, J Biol Chem, 286 (2011) 40614-40623.
[62] K.D. Swanson, M.W. Ratzloff, D.W. Mulder, J.H. Artz, S. Ghose, A. Hoffman, S. White, O.A. Zadvornyy, J.B. Broderick, B. Bothner, P.W. King, J.W. Peters, [FeFe]-hydrogenase oxygen inactivation is initiated at the H cluster 2Fe subcluster, J Am Chem Soc, 137 (2015) 1809-1816.
[63] M.W. Adams, The structure and mechanism of iron-hydrogenases, Biochim Biophys Acta, 1020 (1990) 115-145.

[64] W. Roseboom, A.L. De Lacey, V.M. Fernandez, E.C. Hatchikian, S.P. Albracht, The active site of the [FeFe]-hydrogenase from *Desulfovibrio desulfuricans*. II. Redox properties, light sensitivity and CO-ligand exchange as observed by infrared spectroscopy, J Biol Inorg Chem, 11 (2006) 102-118.
[65] S. Morra, M. Arizzi, F. Valetti, G. Gilardi, Oxygen Stability in the New [FeFe]-Hydrogenase from *Clostridium beijerinckii* SM10 (CbA5H), Biochemistry, (2016).
[66] A.L. De Lacey, V.M. Fernandez, M. Rousset, R. Cammack, Activation and inactivation of hydrogenase function and the catalytic cycle: spectroelectrochemical studies, Chem Rev, 107 (2007) 4304-4330.
[67] R.C. Prince, M.W. Adams, Oxidation-reduction properties of the two Fe4S4 clusters in *Clostridium pasteurianum* ferredoxin, J Biol Chem, 262 (1987) 5125-5128.
[68] E.T. Smith, D.W. Bennett, B.A. Feinberg, Redox properties of 2[4Fe-4S] ferredoxins, Anal. Chim. Acta, 251 (1991) 27-33.
[69] W. Nitschke, M.J. Russell, Redox bifurcations: mechanisms and importance to life now, and at its origin: a widespread means of energy conversion in biology unfolds, Bioessays, 34 (2012) 106-109.
[70] J.W. Peters, D.N. Beratan, G.J. Schut, M.W.W. Adams, On the nature of organic and inorganic centers that bifurcate electrons, coupling exergonic and endergonic oxidation-reduction reactions, Chem Commun (Camb), 54 (2018) 4091-4099.
[71] F. Baymann, B. Schoepp-Cothenet, S. Duval, M. Guiral, M. Brugna, C. Baffert, M.J. Russell, W. Nitschke, On the Natural History of Flavin-Based Electron Bifurcation, Front. Microbiol., 9 (2018) 1357.